Pure Appl. Chem., Vol. 83, No. 2, pp. 269–279, 2011.
doi:10.1351/PAC-CON-10-06-11

Electrochemical nanogravimetric studies of adsorption, deposition, and dissolution processes occurring at platinum electrodes in acid media*

György Inzelt‡, Balázs B. Berkes, and Ákos Kriston

Department of Physical Chemistry, Institute of Chemistry, Eötvös Loránd University, 1117 Budapest, Pázmány Péter sétány 1/A, Hungary

Abstract: Polycrystalline smooth and platinized platinum electrodes have been extensively employed in electrochemistry. It is of utmost importance to gain a deeper insight into the processes occurring during their electrochemical transformations. Piezoelectric nanogravimetry by using electrochemical quartz crystal nanobalance (EQCN) is one of the most powerful tools for obtaining information on the events occurring at the electrode surface. This method has been exploited to monitor the surface mass changes as a function of the electrode potential varying the experimental conditions (time scale, solution composition, temperature), which allows one to draw conclusions in respect of the formation and removal of adsorbed and deposited species as well as changes in the electrochemical double layer. Furthermore, platinum dissolution processes, which are of importance (e.g., regarding the long-term stability of proton exchange fuel cells), are also discussed.

Keywords: adsorption; dissolution; electrochemical quartz crystal nanobalance; platinum electrodes; underpotential deposition.

INTRODUCTION

Platinum electrodes are widely used in electrochemistry and electroanalytical chemistry as an inert electrode in redox reactions because the metal is most stable in aqueous and nonaqueous solutions in the absence of complexing agents, as well as because of its electrocatalytic activity [1–6]. The inertness of the metal does not mean that no surface layers are formed. The true double-layer (ideally polarizable electrode) behavior is limited to ca. 200–300 mV potential interval depending on the crystal structure and the actual state of the metal surface. At low potentials (from ca. 0.3 V vs. SHE and below) the underpotential deposition (upd) of hydrogen takes place. This is a spontaneous dissociation (dissociative chemisorption) of H_2 molecule at Pt resulting in the formation of Pt–H species

$$Pt + H_2 \rightleftarrows 2Pt - H \tag{1}$$

Owing to the not too high Pt–H bond energy, the exchange current of the following electrode reaction

$$H_2 + 2H_2O \rightleftarrows 2H_3O^+ + 2e^- \qquad E^\ominus = 0\ V \tag{2}$$

*Paper based on a presentation made at the 2nd Regional Symposium on Electrochemistry: South East Europe (RSE SEE-2), Belgrade, Serbia, 6–10 June 2010. Other presentations are published in this issue, pp. 253–358.

‡Corresponding author

is high and the electrode process is electrochemically reversible. It is the very reason why the hydrogen electrode is widely used as a reference electrode, and the standard hydrogen electrode (SHE) has been chosen as the primary standard in electrochemistry [7,8]. The standard potential of an electrode reaction (standard electrode potential) is defined as the value of the standard potential of a cell reaction when that involves the oxidation of molecular hydrogen to solvated (hydrated) protons (hydrogen ions) according to eq. 2. The standard state is the hypothetical ideal solution of molality 1 mol kg^{-1} (or the relative activity of H_3O^+, $a_{H_3O^+} = 1$) at standard pressure. The standard pressure is 1 bar (earlier 1 atm = 1.01325 bar, however, the shift is only 0.00026 V at the potential scale). By definition, the potential of this electrode is zero. Although the standard potential should not depend on the material of the metal, the SHE exclusively contains a platinum wire or a platinum sheet covered with platinum black (platinized platinum). Reaction 1 is responsible for the high catalytic activity of platinum both for hydrogen evolution and oxidation as well as hydrogenation reactions since due to the spontaneous splitting of the H_2 molecule, substantial energy is saved.

At high potentials (ca. 0.6 V vs. SHE and above) oxygen adsorption (upd) occurs, resulting in the formation of different platinum hydroxide and oxide species at the platinum surface

$$Pt–OH + H^+ + e^- \rightarrow Pt + H_2O \tag{3}$$

$$PtO + 2H^+ + 2e^- \rightarrow Pt + H_2O \qquad E^\ominus = 0.98\ V \tag{4}$$

$$PtO_2 + 2H^+ + 2e^- \rightarrow PtO + H_2O \qquad E^\ominus = 1.045\ V \tag{5}$$

In its compounds, platinum has oxidation states +2 and +4. The redox reactions—except the formation of hydrides, surface oxides, hydroxides, and metal adatoms (upd of metals)—take place with participation of its complexes, e.g.,

$$PtCl_4^{2-} + 2e^- \rightarrow Pt + 4Cl^- \qquad E^\ominus = 0.758\ V \tag{6}$$

$$PtCl_6^{2-} + 4e^- \rightarrow Pt + 6Cl^- \qquad E^\ominus = 0.744\ V \tag{7}$$

For the study of the changes occurring at the platinum electrode surface several methods, among others electrochemical quartz crystal nanobalance (EQCN) [9–29], radiotracer [31–36], probe beam deflection [37], Fourier transform infrared (FTIR) [38,39] and Raman [40] spectroscopies, sum frequency generation [41], synchrotron X-ray scattering [42], contact electric resistance [43], and potentiodynamic electrochemical impedance measurements [44] have been applied. In this paper, we report the recent results obtained by using EQCN. The details of the experiments have been described in our previous papers [28,29]. With the help of this method, the total changes of the surface mass can be monitored, which allows us to draw conclusions regarding the surface events. However, the experimental evidence revealed by using other techniques should also be taken into account in order to elucidate the total mass change measured. Especially, the results of radiotracer and spectroscopic measurements supply valuable information concerning the ion sorption and the adsorption of water on the platinum surface. The piezoelectric nanogravimetry by using EQCN is a very powerful tool, however, the variation of the frequency of the oscillating quartz also depends on other factors, most notably on the density and viscosity of the contacting liquid [10,11,28,29]. We will show that this effect can be separated, and reliable data can be obtained for the variation of the surface mass as a function of different parameters.

VOLTAMMETRIC BEHAVIOR OF PLATINUM ELECTRODES AND THE VARIATIONS OF SURFACE MASS

Underpotential deposition of hydrogen and oxygen

The typical voltammetric curve used generally for the presentation of hydrogen and oxygen adsorption on polycrystalline platinum and the simultaneously detected mass change are shown in Fig. 1.

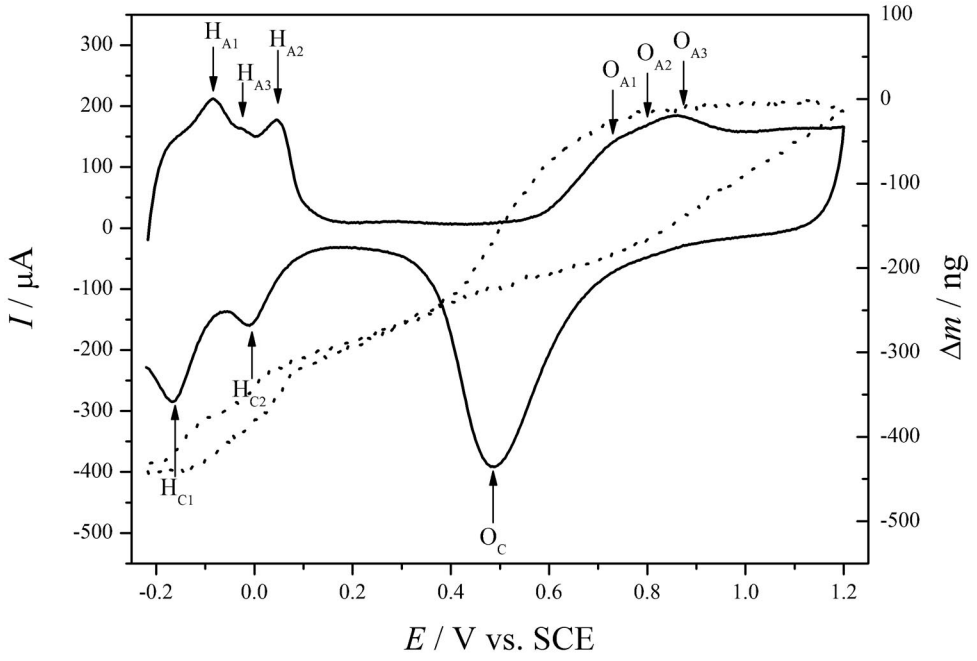

Fig. 1 Cyclic voltammograms (continuous line) and simultaneous changes of surface mass (Δm) derived from the EQCN frequency changes (dotted line) for a platinum electrode in contact with 1 mol dm^{-3} H_2SO_4 at 20 °C. Scan rate: 10 mV s^{-1}.

The shape of the curve depends on the nature of the anion(s) present in the system. In reality there is an overall behavior reflecting simultaneous H/O and anion adsorption. In the case of polycrystalline platinum, three anodic waves appear due to the oxidation of the adsorbed hydrogen according to the reaction

$$\text{Pt–H} \rightleftarrows \text{Pt} + \text{H}^+ + \text{e}^- \tag{8}$$

indicating at least three different states of the adsorbed hydrogen. The different peak potentials are related to different bonding energies, i.e., there are energetically different surface sites. The adsorption–desorption processes are reversible, however, only two cathodic waves are observed. The formation of Pt–OH, PtO, and PtO_2 species are irreversible, no distinct peaks can be detected, which is related to the continuous transformation of the surface oxide and a place-exchange between the Pt and O atoms. Usually, a single reduction peak can be observed, however, there are indications in the literature for the overlap of the oxide and hydrogen regions of platinum electrodes in aqueous acid solution [45]. At least three distinct hydrous oxide reduction peaks (or regions) were observed, and in some cases one of these peaks commenced at ca. 0.0 V, i.e., it was almost totally within the hydrogen gas evolution region. Repeated hydrous oxide growth and reduction, which disrupt and thus activate the metal surface, strongly influence the electrocatalytic processes occurring on platinum at low potentials.

The mass increase in the hydrogen upd region cannot be assigned to the removal of adsorbed hydrogen since it would cause a mass decrease, albeit a small one due to the small molar mass of the hydrogen. This mass increase is related to the adsorption of water molecules and anions as the adsorbed hydrogen is oxidized in acid media. The adsorption of these species continues in the double-layer region. The surface coverage (θ) of HSO_4^- and SO_4^{2-} ions reaches a maximum value of $0.05 < \theta < 0.2$ [3,22,33,34] at ca. E = 0.95 V vs. SCE depending on the experimental conditions. There is a slight

desorption of anions as the oxide layer forms. The mass increase in the oxide region corresponds to the attachment of oxygen atoms to the platinum.

Cation adsorption and underpotential deposition

The adsorption of cations is expected at lower (less positive) potentials than the potential of zero charge (pzc). However, in acid solutions or solutions containing alkali metal ions or Mg^{2+} ions, specific adsorption has not been observed. The only exception is the Cs^+ ion when both the radiotracer

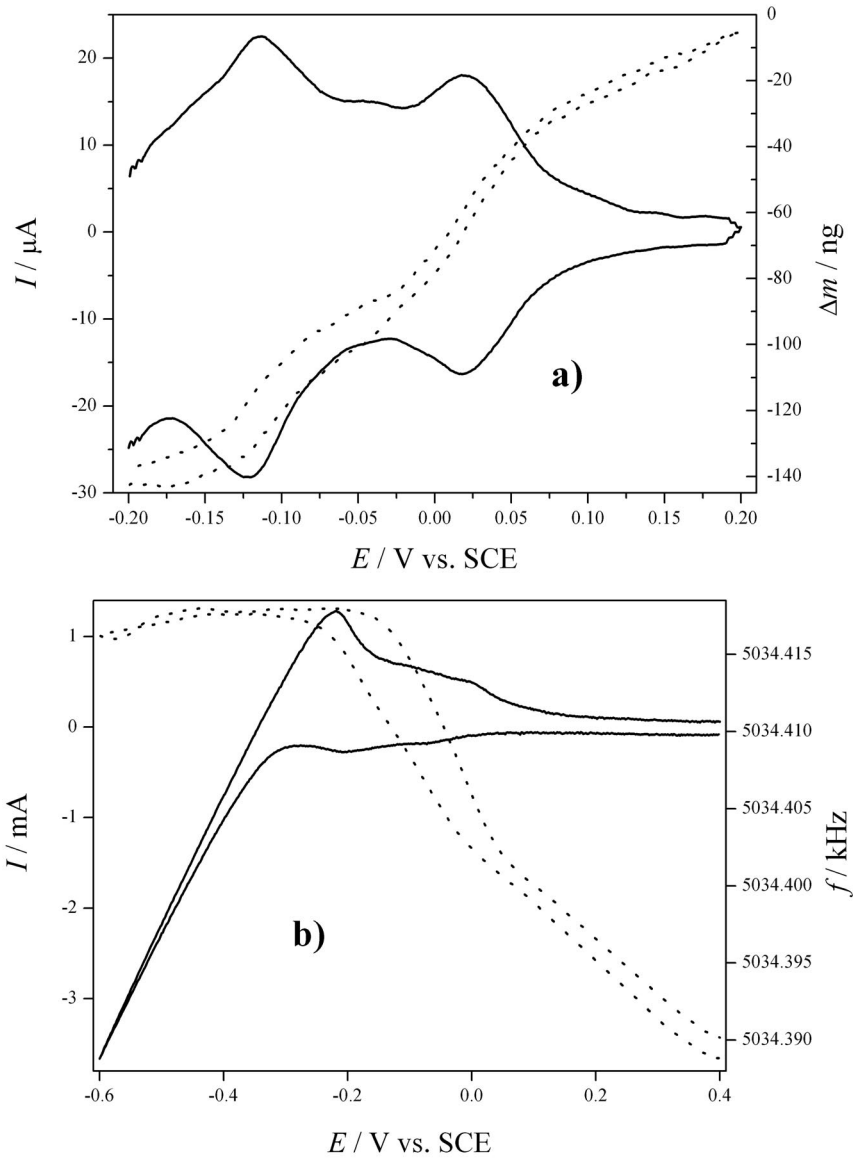

Fig. 2 Cyclic voltammograms (continuous lines) and simultaneous changes of surface mass (Δm) derived from the EQCN frequency changes (dotted line) for a platinum electrode in contact with 1 mol dm^{-3} H_2SO_4 at 0 °C, scan rate: 1 mV s^{-1} (a) and the frequency change (dotted line) in 1 mol dm^{-3} H_2SO_4–K_2SO_4 solution (pH 2) at 20 °C, scan rate: 10 mV s^{-1} (b), respectively.

[30,31,35] and EQCN [29] results revealed the existence of such phenomenon. The mass change in the hydrogen upd region for a platinum electrode immersed in 1 mol dm^{-3} H_2SO_4 is shown in Fig. 2a. The EQCN frequency response obtained in the hydrogen evolution and upd regions for a platinum electrode in contact with H_2SO_4–K_2SO_4 (pH 2) solution is displayed in Fig. 2b.

According to eq. 8, the hydrogen oxidation–reduction reaction is pH-dependent, therefore, a 60 mV/pH shift in the peak potentials is expected and is seen in Fig. 3a. The frequency excursion as a function of potential remains practically the same despite the fact that due to the large change of the density and viscosity of the solutions a large frequency shift (more than –400 Hz in the concentration range from 0.1 to 4 mol dm^{-3} H_2SO_4) occurs (Figs. 3b,c). In Fig. 3b, the total frequency changes related to the increase of density and viscosity are illustrated, while in Fig. 3c the variations of Δf vs. E functions are displayed, as the concentration of H_2SO_4 was increased. In Fig. 3c, the curves were shifted arbitrarily for the sake of the better visibility of the frequency changes as a function of potential.

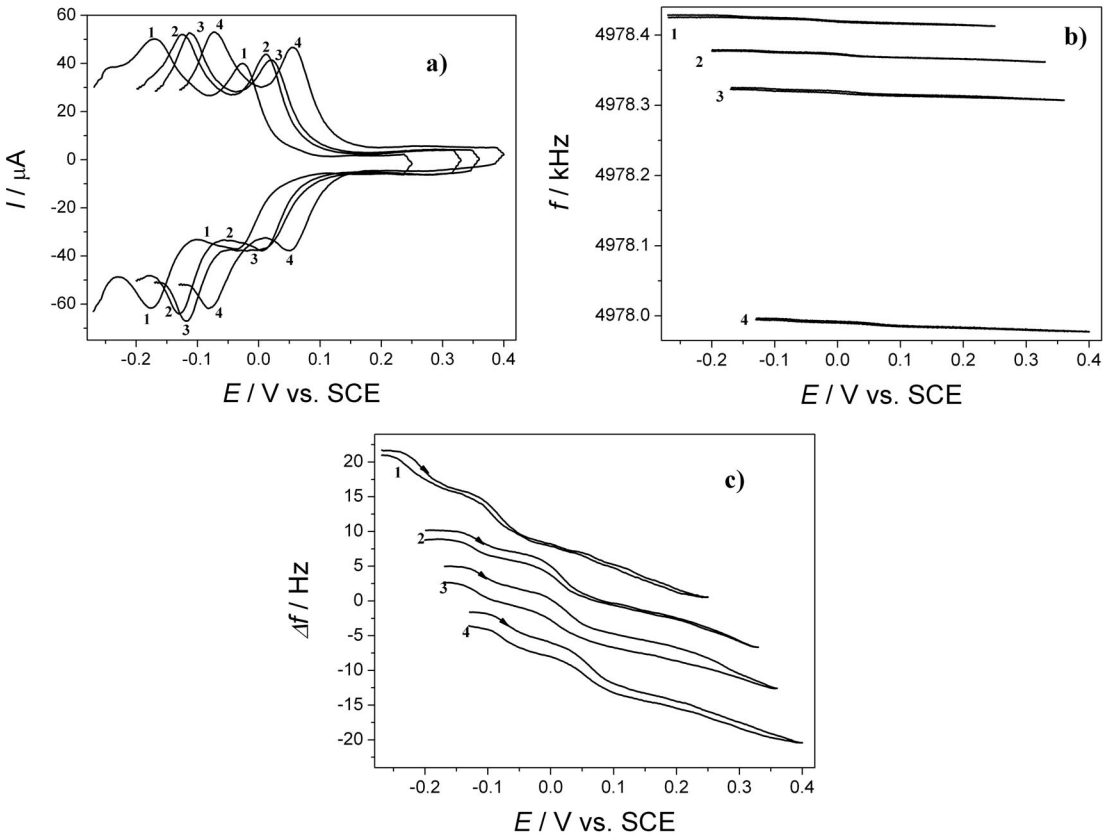

Fig. 3 Effect of the concentration of sulfuric acid on the cyclic voltammetric (a) and simultaneously detected EQCN frequency (b) responses at a platinized platinum electrode in contact with (1) 0.1, (2) 0.5, (3) 1, and (4) 4 mol dm^{-3} H_2SO_4. The respective Δf vs. E plots (c). Scan rate: 2 mV s^{-1}. (1 Hz = 9 ng.) (Adapted with permission from the original version in ref. [29]. Copyright © 2010, Elsevier.)

The adsorption of Cs^+ ions manifests itself in a much higher frequency change in the hydrogen upd region than that expected from the density and viscosity effect alone as well as the deviation of the frequency changes that usually can be observed in the hydrogen upd and the double-layer regions as

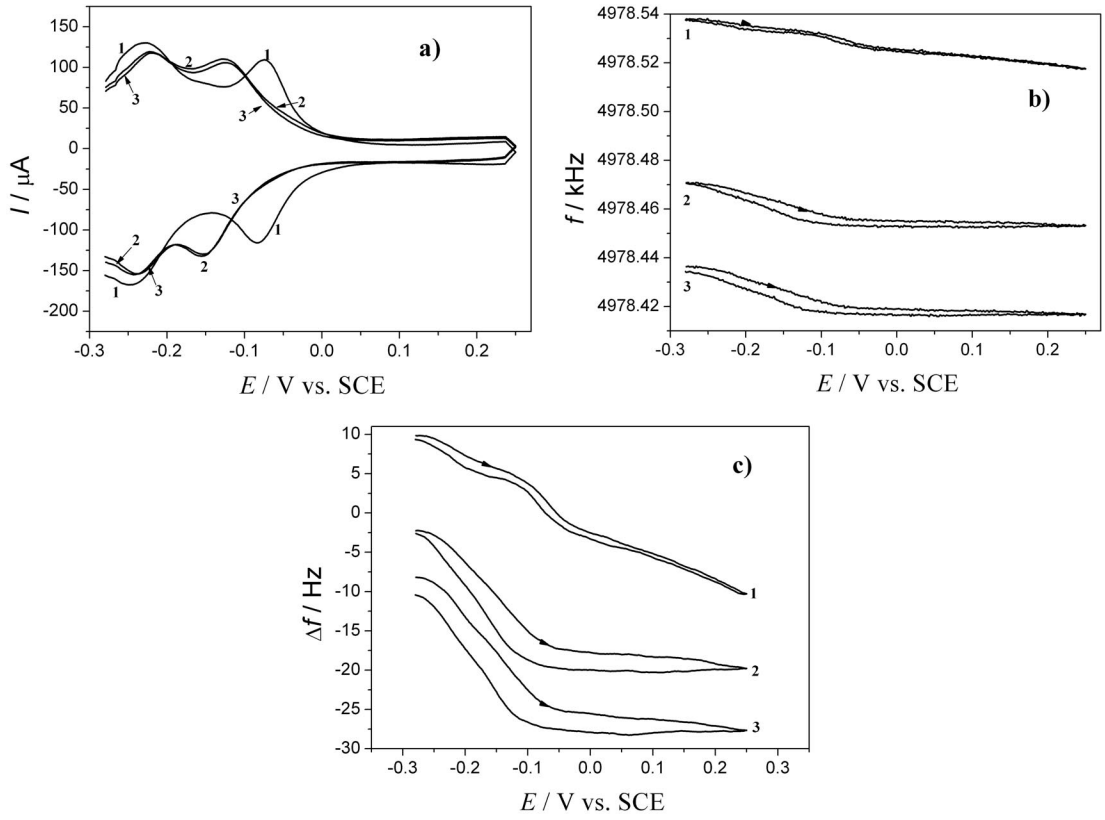

Fig. 4 Effect of the concentration of Cs_2SO_4 on the cyclic voltammetric (a) and simultaneously detected EQCN frequency (b) responses for the electrode used in the experiments shown in Fig. 3 in contact with (1) 0.0, (2) 0.1, and (3) 0.136 mol dm^{-3} Cs_2SO_4. The respective Δf vs. E plots (c). Scan rate: 5 mV s^{-1}. Sulfuric acid concentrations and the pH values were as follows: (1) 0.05, (2) 0.14 and (3) 0.127 mol dm^{-3}; pH: (1) 1.56, (2) 1.16 and (3) 1.38. (Adapted with permission from the original version in ref. [29]. Copyright © 2010, Elsevier.)

illustrated in Fig. 4. Figure 4b shows the total frequency changes, while Fig. 4c shows the Δf vs. E functions where the frequency variations with potential are better seen.

In fact, there is a competitive adsorption between the H^+ and Cs^+ ions, and an increase of the concentration of Cs^+ ions results in a decrease of the amount of adsorbed hydrogen. For the highest Cs^+–H^+ concentration ratio, $\theta = 0.12$ was calculated with respect to the Cs^+ ions [29]. Owing to the presence of the excess Cs^+ ions on the surface, an induced anion adsorption occurs in the hydrogen upd region. The desorption of Cs^+ ions takes place in the double-layer region.

For many cations, the investigation of the adsorption is prevented since upd of several cations occurs in the potential range between the hydrogen and oxygen evolutions. Figure 5 shows the upd of zinc, which takes place in the hydrogen upd region. The mass change is due to the deposition–dissolution of zinc atoms together with a small amount of anions [36].

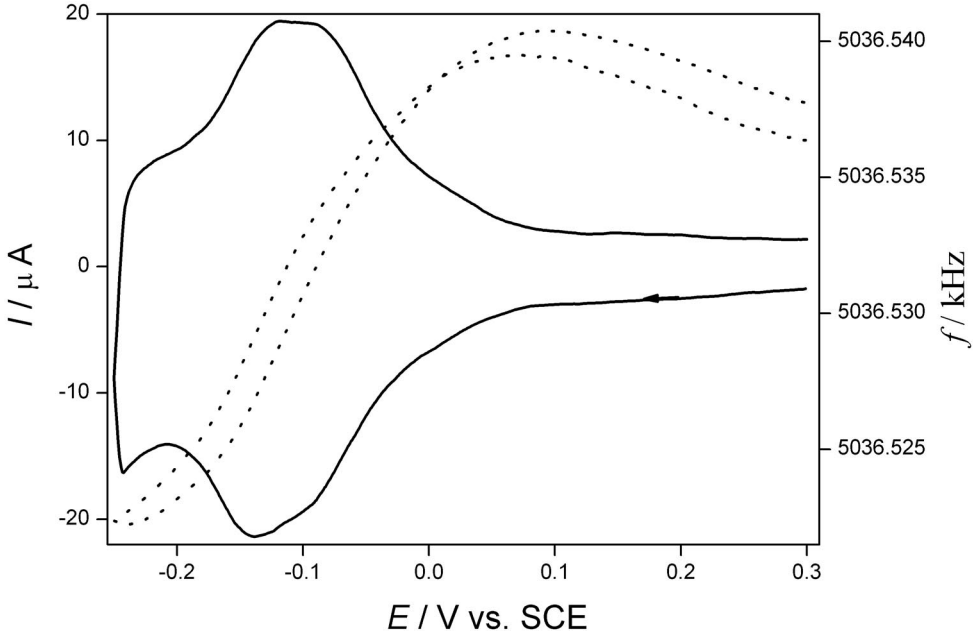

Fig. 5 Cyclic voltammogram (continuous line) and simultaneously obtained EQCN frequency change (dotted line) for a smooth platinum electrode in contact with solution of 0.05 mol dm^{-3} H_2SO_4 and 0.012 mol dm^{-3} $ZnSO_4$ at 20 °C. Scan rate is 1 mV s^{-1}. (1 Hz = 9 ng.)

Anion adsorption

The adsorption of anions is a widely studied phenomenon. There is direct evidence for the anion adsorption on platinum based on the results of radiotracer, EQCN, and spectroscopic measurements. In the case of specifically adsorbed ions the shape of the cyclic voltammograms also changes. It has been established that I^-, Br^-, and Cl^- are strongly adsorbed on platinum, but there is a specific adsorption of phosphate and sulfate ions, too. The strength of the adsorption can easily be shown by using radiotracer labeling since the more strongly adsorbed anions replace the anions, which have a weaker bonding to platinum atoms, on the electrode surface [32–35]. The adsorption of the perchlorate ions is the weakest, however, ClO_4^- ions can undergo a reduction at platinum electrodes, and the reaction product, the Cl^- ions adsorb on the platinum surface. The distortion of the voltammetric curves in the presence of ClO_4^- ions is firm evidence for the occurrence of the reduction process [3]. The adsorption of anions also affects the formation of the oxide layer, the strong anionic adsorption hinders this process, which consequently starts at more positive potentials. The EQCN technique supplies information only on the variation of the total surface mass, which involves the contribution of adsorbed water and in the case of Cs^+ ions also that of these ions. The radiotracer method, using labelled anions, is an adequate tool to follow anion adsorption in the course of voltammetric measurements, and to gain simultaneous information on hydrogen and anion adsorption [3,32–35]. The use of EQCN and radiotracer techniques is supplementary, because the latter method can only be applied in dilute solutions.

The differential voltradiometric curve ($\Delta\Gamma/\Delta E$ vs. E) and the voltammetric curves (which were measured in the presence of 1.7×10^{-3} mol dm^{-3} $H_2{}^{35}SO_4$ in 1 mol dm^{-3} $HClO_4$) were compared in refs. [3,33]. From the comparison of these curves, it was stated that the position of the anion adsorption peaks in the hydrogen adsorption region is not far from those of the hydrogen adsorption.

Similar representation of the differential voltmassogram derived from the EQCN frequency curve is shown in Fig. 6.

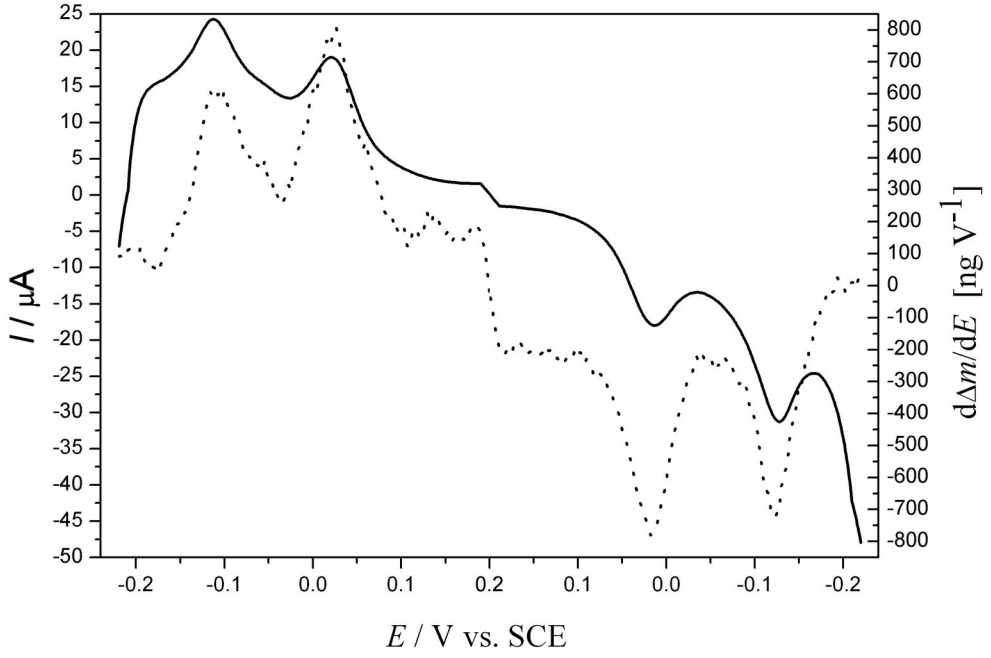

Fig. 6 Differential voltmassogram (dΔm/dE vs. E curve) (dotted line) and voltammogram (continuous line) for a platinum electrode in contact with 1 mol dm^{-3} H_2SO_4 at 20 °C. Scan rate: 1 mV s^{-1}.

Albeit the parallelism is striking, the oxidation current (charge) belongs to the oxidation of adsorbed hydrogen (or during the reduction, the discharge of hydrogen ions) and there is only a partial replacement of the removed hydrogen ions by anions and water molecules.

Formation, rearrangement, and reduction of oxide layer

It is well known that platinum can undergo dissolution at high anodic potentials in the presence of complexing agents, such as Cl^- ions. In this case, a high anodic current and a substantial mass loss can be observed. However, recently it has been evident that at elevated temperatures an anodic dissolution can be observed even in the absence of any complexing agent [28] as illustrated in Fig. 7.

Even more remarkable, there is also a dissolution during the cathodic cycle, which has been proven recently [28]. A mass loss occurs during the reduction of the oxide layer due to the removal of oxygen atoms from the surface, however, in addition a permanent surplus mass loss also appears at the end of the reduction process, which indicates the dissolution of a certain amount of platinum as seen in Fig. 8.

This effect can be explained by the place exchange process between the surface platinum and oxygen atoms. It follows that a certain number of platinum atoms will not be strongly bounded to the underlying platinum atoms [4,25,42], and will go into the solution phase during reduction. Alternatively, platinum ions during the reduction of PtO_2 formed at 1.3 V will be dissolved according to the following scheme [27,46,47]:

$$PtO_2 + 4H^+ + 2(2 - x)e^- \rightarrow xPt^{2+} + (1 - x)Pt + 2H_2O \quad (9)$$

The occurrence of this process strongly depends on the time scale (scan rate) and the positive potential limit, therefore, a certain amount of time is needed for the place exchange process to be completed or the PtO_2 to be formed. The extent of the platinum loss is much smaller than that in the usual

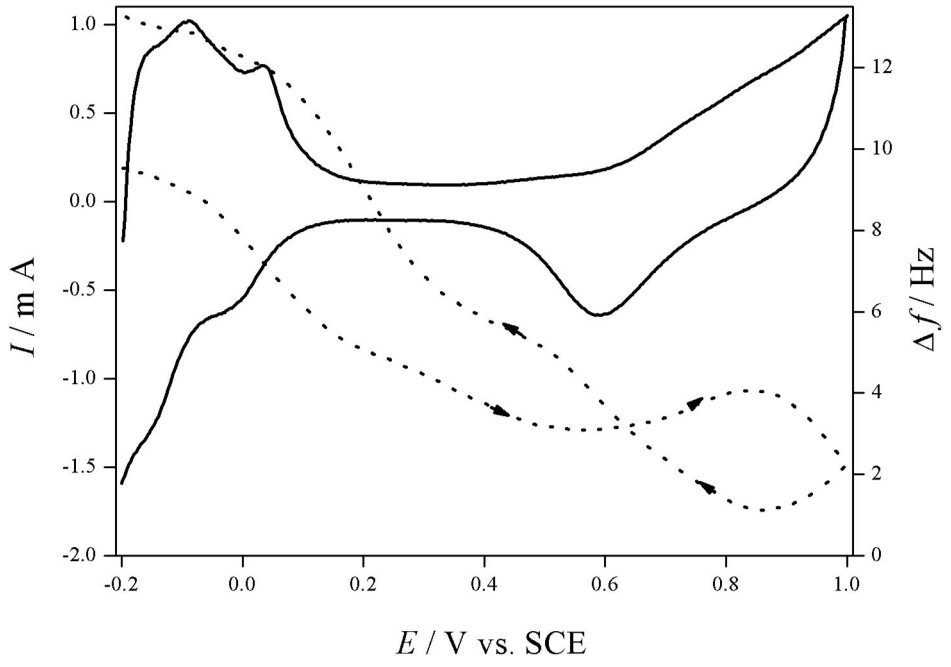

Fig. 7 Cyclic voltammogram (continuous line) and simultaneously obtained EQCN frequency changes (dotted line) for a platinized platinum electrode in contact with a solution containing 0.5 mol dm^{-3} H_2SO_4 at 60 °C. Scan rate: 20 mV s^{-1}. (1 Hz = 9 ng.)

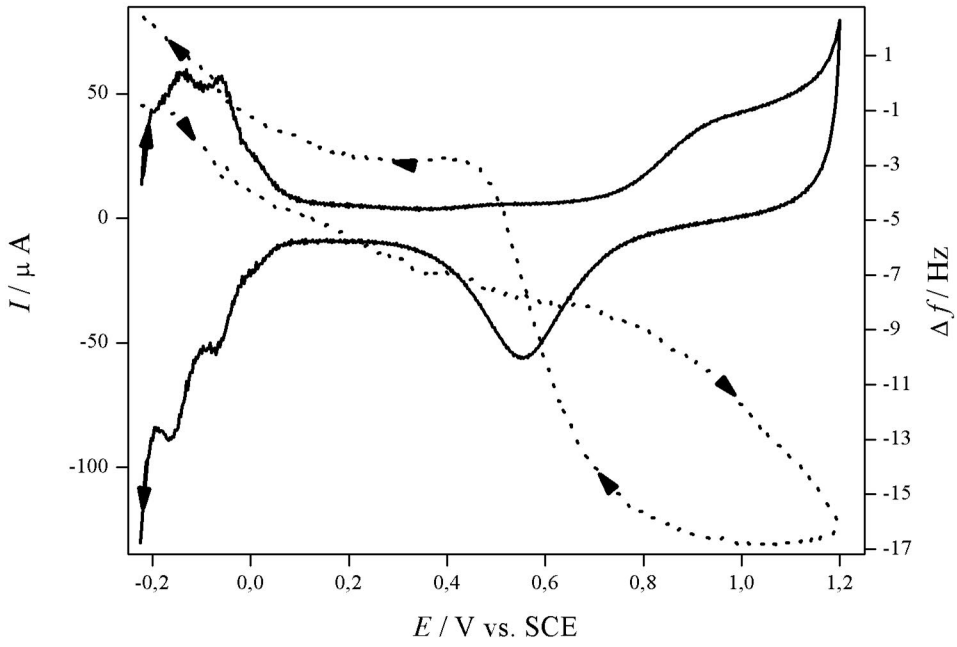

Fig. 8 Cyclic voltammogram (continuous line) and simultaneously obtained EQCN frequency change (dotted line) for a platinum electrode in contact with 0.5 mol dm^{-3} H_2SO_4 at 20 °C. Scan rate: 5 mV s^{-1}. (1 Hz = 9 ng.) (Adapted with permission from the original version in ref. [28]. Copyright © 2010, Elsevier.)

anodic dissolution, however, during extensive cycling it will become substantial. This finding may also explain the dissolution and redeposition of platinum catalyst that has been observed in fuel cells, since the potential usually changes in this potential region during variable loading, e.g., in a vehicle.

CONCLUSIONS

Although platinum electrode is often considered as a thoroughly characterized system, there are still several properties, which have to be investigated to gain a better understanding of the processes determining its behavior. This is of utmost importance because polycrystalline platinum is widely used not only in laboratories in many electrochemical experiments but also in power sources (e.g., in fuel cells) and electrolytic cells. Based mostly on the systematic EQCN investigations carried out by the authors, the surface processes such as adsorption of ions and water molecules, upd of hydrogen, oxygen, and metals as well as two types of dissolution processes are discussed.

From these results, taking into account the data obtained by radiotracer and spectroscopic techniques, the following conclusions can be drawn.

Specific adsorption of most of the cations, e.g., Na^+, K^+, and Mg^{2+}, cannot be detected except that of the Cs^+ ions. The results of the EQCN technique supply evidence for the competitive adsorption of Cs^+ and H^+ ions in the hydrogen evolution and hydrogen upd regions. The upd of metal ions can be detected with great accuracy, however, it prevents obtaining information on the specific adsorption of those ions, which occurs at more negative potentials than the pzc of the platinum. The adsorption of water molecules—if any—does not change in the hydrogen upd region, however, it certainly takes place during the oxidation of the adsorbed hydrogen and also in the double-layer region. The adsorption of anions also starts simultaneously with the oxidation of the adsorbed hydrogen, and the amount of the adsorbed anions increases in the double-layer region. In the oxide region, a desorption of the anions takes place. The recent EQCN studies reveal two practically important phenomenena (i.e., the anodic dissolution of platinum) even in the absence of complexing agents at elevated temperatures, and a platinum loss during the electroreduction of the platinum oxide.

ACKNOWLEDGMENTS

The financial support of the National Office of Research and Technology (OMFB-00356/2007 and OM-00121-00123/2008) and National Scientific Research Fund (OTKA K71771) as well GVOP-3.2.1-2004-040099 is acknowledged.

REFERENCES

1. R. Woods. In *Electroanalytical Chemistry*, Vol. 9, A. J. Bard (Ed.), pp. 1–162, Marcel Dekker, New York (1976).
2. J. F. Llopis, I. Colom. In *Encyclopedia of Electrochemistry of Elements*, Vol. 6, A. J. Bard (Ed.), pp. 170–219, Marcel Dekker, New York (1976).
3. G. Horányi, G. Inzelt. In *Encyclopedia of Electrochemistry*, Vol. 7a, F. Scholz, C. J. Pickett, A. J. Bard, M. Stratmann (Eds.), pp. 497–528, Wiley-VCH, Weinheim (2006).
4. P. A. Christensen, A. Hamnett. *Techniques and Mechanisms in Electrochemistry*, pp. 228–287, Blackie Academic, London (1994).
5. R. Borup, J. Meyers, B. Pivovar, Y. S. Kim, R. Mukundan, N. Garland, D. Myers, M. Wilson, F. Garzon, D. Wood, P. Zelenay, K. More, K. Stroh, T. Zawodzinski, J. Boncella, J. E. McGrath, M. Inaba, K. Miyatake, M. Hori, K. Ota, Z. Ogumi, S. Miyata, A. Nishikata, Z. Siroma, Y. Uchimoto, K. Yasuda, K. Kimijima, N. Iwashita. *Chem. Rev.* **107**, 3904 (2007).
6. S. Srinivasan. *Fuel Cells*, Springer, New York (2006).

7. E. R. Cohen, T. Cvitas, J. G. Fry, B. Holmström, K. Kuchitsu, R. Marquardt, I. Mills, F. Pavase, M. Quack, J. Stohner, H. L. Strauss, M. Takami, A. J. Thor (Eds.). *IUPAC Quantities, Units and Symbols in Physical Chemistry*, 3rd ed., pp. 70–76, RSC Publishing, Cambridge (2007).
8. R. Parsons. *Pure Appl. Chem.* **37**, 499 (1974).
9. R. P. Buck, E. Lindner, W. Kutner, G. Inzelt. *Pure Appl. Chem.* **76**, 1139 (2004).
10. V. Tsionsky, L. Daikhin, M. Urbakh, E. Gileadi. In *Electroanalytical Chemistry*, A. J. Bard, I. Rubinstein (Eds.), pp. 1–99, Marcel Dekker, New York (2004).
11. M. Hepel. In *Interfacial Electrochemistry*, A. Wieckowski (Ed.), pp. 599–630, Marcel Dekker, New York (1999).
12. R. Schumacher. *Angew. Chem., Int. Ed. Engl*. **29**, 329 (1990).
13. Z. X. Shu, S. Bruckenstein. *J. Electroanal. Chem.* **317**, 263 (1991).
14. C. P. Wilde, M. Zhang. *J. Electroanal. Chem.* **327**, 307 (1992).
15. K. Shimazu, H. Kita. *J. Electroanal. Chem.* **341**, 361 (1992).
16. R. Raudonis, D. Plausinitis, V. Daujotis. *J. Electroanal. Chem.* **358**, 351 (1993).
17. V. I. Birss, M. Chang, J. Segal. *J. Electroanal. Chem.* **355**, 181 (1993).
18. M. Watanabe, H. Uchida, N. Ikeda. *J. Electroanal. Chem.* **380**, 255 (1995).
19. W. Visscher, J. F. E. Gootzen, A. P. Cox, J. A. R. Van Veen. *Electrochim. Acta* **43**, 533 (1998).
20. F. Gloaguen, J.-M. Léger, C. Lamy. *J. Electroanal. Chem.* **467**, 186 (1999).
21. B. Gollas, J. M. Elliot, P. N. Barlett. *Electrochim. Acta* **45**, 3711 (2000).
22. M. C. Santos, D. W. Miwa, S. A. S. Machado. *Electrochem. Commun.* **2**, 692 (2000).
23. C. P. Wilde, S. V. De Cliff, K. C. Hui, D. J. L. Brett. *Electrochim. Acta* **45**, 3649 (2000).
24. B. E. Conway, A. Zolfaghari, W. G. Pell, G. Jerkiewicz. *Electrochim. Acta* **48**, 3775 (2003).
25. G. Jerkiewicz, G. Vatankhah, J. Lessard, M. P. Soriaga, Y.-S. Park. *Electrochim. Acta* **49**, 1451 (2004).
26. V. A. T. Dam, F. A. de Bruijn. *J. Electrochem. Soc.* **154**, B494 (2007).
27. A. P. Yadav, A. Nishikata, T. Tsuru. *Electrochim. Acta* **52**, 7444 (2007).
28. G. Inzelt, B. B. Berkes, A. Kriston. *Electrochim. Acta* **55**, 4742 (2010).
29. B. B. Berkes, A. Szekely, G. Inzelt. *Electrochem. Commun.* **12**, 1095 (2010).
30. A. N. Frumkin, O. A. Petrii, I. G. Schchigorev, V. A. Safonov. *Z. Phys. Chem.* **243**, 261 (1970).
31. T. Ya. Kolotyrkina, O. A. Petrii, V. E. Kazarinov. *Elektrokhimiya* **10**, 1352 (1974).
32. G. Horányi, G. Inzelt. *J. Electroanal. Chem.* **86**, 215 (1978).
33. G. Horányi, E. Rizmayer. *J. Electroanal. Chem.* **218**, 337 (1987).
34. G. Horányi. In *Radiotracer Studies of Interfaces*, G. Horányi (Ed.), pp. 39–98, Elsevier, Amsterdam (2004).
35. A. Wieckowski. In *Modern Aspects of Electrochemistry*, Vol. 21, R. E. White, J. O'M. Bockris, B. E. Conway (Eds.), pp. 65–119, Plenum, New York (1990).
36. G. Horanyi, A. Aramata. *J. Electroanal. Chem.* **434**, 201 (1997).
37. E. D. Bidoia, F. McLarnon, E. J. Cairns. *J. Electroanal. Chem.* **482**, 75 (2000).
38. A. Berná, J. M. Feliu, L. Gancs, S. Mukerjee. *Electrochem. Commun.* **11**, 1695 (2008).
39. D.-M. Zeng, Y.-X. Jiang, Z.-Y. Zhou, Z.-F. Su, S.-G. Sun. *Electrochim. Acta* **55**, 2065 (2010).
40. B. Ren, X. Xu, X. Q. Li, W. B. Cai, Z. Q. Tian. *Surf. Sci.* **427–428**, 157 (1999).
41. H. Noguchi, T. Okada, K. Uosaki. *Electrochim. Acta* **53**, 6841 (2008).
42. Z. Nagy, H. You. *Electrochim. Acta* **47**, 3037 (2002).
43. V. A. Marichev. *Electrochem. Commun.* **10**, 643 (2008).
44. G. A. Ragoisha, N. P. Osipovich, A. S. Bondarenko, J. Zhang, S. Kocha, A. Iiyama. *J. Solid State Electrochem.* **14**, 531 (2010).
45. L. D. Burke, A. J. Ahern. *J. Solid State Electrochem.* **5**, 553 (2001).
46. M. Ueda, Y. Kuwahara, A. Nakazawa, M. Inoune. *J. Phys. Chem. C* **113**, 15707 (2009).
47. D. R. Johnson, D. T. Napp, S. Bruckenstein. *Electrochim. Acta* **15**, 1493 (1970).

